Surface CO_2 leakage during the first shallow subsurface CO_2 release experiment

J.L. Lewicki[1], C.M. Oldenburg[1], L. Dobeck[2], and L. Spangler[2]

[1] Earth Sciences Division, Lawrence Berkeley National Laboratory, 1 Cyclotron Rd., MS 90-1116, Berkeley, CA 94720 USA, jllewicki@lbl.gov

[2]Department of Chemistry and Biochemistry, Montana State University, 108 Gaines Hall, PO Box 173400, Bozeman, MT, 59717 USA

Abstract. A new field facility was used to study CO_2 migration processes and test techniques to detect and quantify potential CO_2 leakage from geologic storage sites. For 10 days starting 9 July 2007, and for seven days starting 5 August 2007, 0.1 and 0.3 t CO_2 d^{-1}, respectively, were released from a ~100-m long, sub-water table (~2.5-m depth) horizontal well. The spatio-temporal evolution of leakage was mapped through repeated grid measurements of soil CO_2 flux (F_{CO2}). The surface leakage onset, approach to steady state, and post-release decline matched model predictions closely. Modeling suggested that minimal CO_2 was taken up by groundwater through dissolution, and CO_2 spread out on top of the water table. F_{CO2} spatial patterns were related to well design and soil physical properties. Estimates of total CO_2 discharge along with soil respiration and leakage discharge highlight the influence of background CO_2 flux variations on detection of CO_2 leakage signals.

1. Introduction

As geologic carbon sequestration gains momentum as a viable strategy to mitigate climate change associated with elevated CO_2 concentrations in the atmosphere, the number of large, industrial-scale and smaller-scale pilot CO_2 injection projects has increased [e.g., *International Energy Agency*, 1997, 2004; *IPCC*, 2005]. While the purpose of geologic carbon sequestration is to trap CO_2 underground, CO_2 has the potential to leak from the storage site along permeable pathways such as well bores or faults to the near-surface environment. The technical community must therefore demonstrate the ability to detect, characterize, mitigate, and remediate CO_2 leakage from geologic CO_2 storage sites to

satisfy public concerns about safety and environmental impact of geologic CO_2 storage. In particular, near-surface detection of CO_2 leakage could be challenging due to the large variation in natural background CO_2 fluxes arising from biological processes [e.g., *Lewicki et al.*, 2005]. A new facility was recently built in an agricultural field at Montana State University by the Zero Emissions Research and Technology (ZERT) Project to release CO_2 into the shallow subsurface from point and line sources that emulate leakage along, e.g., abandoned wells or faults. This is to our knowledge the first facility that provides the opportunity to study CO_2 migration processes and to test techniques to detect and quantify potential CO_2 leakage from geologic storage sites.

In July and August 2007, two controlled releases of CO_2 were carried out at different rates from a shallow horizontal well. Changing meteorological conditions and associated soil microclimate and plant phenology over this timeframe led to varying levels of background biological fluxes within which leakage signals evolved. We conducted numerical modeling of the CO_2 releases to elucidate CO_2 migration processes and predict the magnitude and geometry of CO_2 leakage signals. We then carried out detailed measurements of soil CO_2 flux (F_{CO2}) along a grid at varying distances from the well to characterize the spatio-temporal evolution of both CO_2 leakage and background biological (soil respiration) fluxes, and to quantify surface CO_2 leakage rates. Here, we (1) present and compare field measurement and modeling results of what is to our knowledge the first-ever CO_2 shallow-release experiments aimed at studying surface leakage from geologic storage projects, and (2) discuss implications of the results for detection of surface leakage.

2. Field Site and Experimental Design

The CO_2 release experiments were conducted at Montana State University, at the Montana Agricultural Experiment Research Center in Bozeman, MT. The study site was a ~0.12 km^2 nearly flat field, with prairie grasses, alfalfa, and Canadian thistle. Here, a ~30 cm-thick clay topsoil overlies a ~20 cm-thick clayey silt layer, which overlies an alluvial sandy cobble with 10-25 cm diameter cobbles. A N45E-trending horizontal well with a 73-m long central slotted (perforated) section and 15- and 12-m long unslotted sections on the sloping NE and SW ends, respectively, was installed in the field. The slotted section was located at ~1.3-2.5 m depth within the alluvial sandy cobble and was divided into six ~12-m long zones separated by 0.4-m wide inflatable packers (Figure 1a). The water table depth was ~ 1.6 m, resulting in sub-water table CO_2 releases. From 9-19 July 2007 (Release 1), and from 5-10 August 2007 (Release 2), 0.1 t CO_2 d^{-1} and 0.3 t CO_2 d^{-1}, respectively, were released from the well evenly from each of the six slotted zones. The 0.1 t d^{-1} rate was chosen based on numerical simulations to provide a challenging detection problem while still ensuring that injected CO_2 would reach the ground surface. The 0.3 t d^{-1} rate was chosen to obtain a larger surface flux for demonstration purposes.

2. Methods

The simulator TOUGH2/EOS7CA [*Pruess et al.*, 1999; *Oldenburg and Unger*, 2003; 2004] for modeling subsurface migration of water, CO_2, and air is used to model CO_2 releases into the shallow subsurface. Properties of the two-dimensional (2D) model oriented transverse to the horizontal well are shown in Table 1. In all cases, the initial condition is a gravity-capillary steady state with zero rainfall infiltration, constant pressure at the top and bottom, and no groundwater flow. Note the larger moisture retention capacity of the soil leads to an initial condition with a capillary barrier at the soil-cobble interface. A shallow vertical-well CO_2 injection test was conducted at the field site in October 2006 to observe injectivity and surface CO_2 flux of the soil-cobble system. Accumulation chamber measurements of F_{CO2} for this test were used as constraints to fit model permeabilities to the two-layer soil-cobble system. The high calibrated permeability of the soil (Table 1) likely arises from cracks and root casts that create macropores through which soil gas and atmospheric air readily flow. Fitted soil and cobble properties were then used in forward models of the two horizontal well releases.

F_{CO2} was measured using a WEST Systems Fluxmeter (WEST Systems, Pisa, Italy) based on the accumulation chamber method [*Chiodini et al*., 1998], with accuracy and repeatability of −12.5% [*Evans et al.*, 2001] and ±10% [*Chiodini et al.*, 1998], respectively. F_{CO2} was measured at 1-m spacing along the surface well trace on 17-18 July, and 7-8 August 2007 (Figure 1), and repeatedly on a daily basis at 2.5 to 10-m spacing on grids from 7-16 July and from 9-12 August 2007 (Figure 2). F_{CO2} measurements were made between 03:00 and 14:00 on any given day. F_{CO2} maps were

interpolated from grid measurements using a minimum curvature spline technique. While this method produces a relatively smooth surface, it remains faithful to the original sample data. Geostatistical interpolation/simulation methods [e.g., *Lewicki et al.*, 2005] were inappropriate for our F_{CO2} datasets due to poor spatial correlation on the grid measurement scale and lack of stationarity. Total CO_2 discharge (D_{tot}) was estimated for each grid dataset by calculating the declustered mean F_{CO2} using GSLIB [*Deutsch and Journel*, 1998] and multiplying it by the total measurement area (7700 m^2).

3. Results

For Release 1, numerical simulations predicted surface breakthrough of CO_2 leakage after 1.5 days (Figure 3). Modeled leakage flux at the surface above the well then reached near-steady state on ~Day 6 of Release 1; however, flux continued to increase very gradually over the remainder of the release period. Simulated leakage flux declined sharply by ~50% over the first day following the end of Release 1, and then declined more gradually to low (near-zero) values by the beginning of Release 2. For Release 2, surface breakthrough was predicted to occur more quickly, and leakage flux above the well was predicted to reach steady state after only ~3 days. The decline in simulated leakage flux was sharp (by >90%) over the first day following the end of Release 2, and then more gradual over subsequent days.

Cross-sections of simulated subsurface CO_2 concentrations and corresponding cross-well profiles of surface CO_2 flux are shown in Supplement 1 for Day 8 of Releases 1 and 2

(i.e., near-steady state conditions). On Day 8 of both releases, mushroom-shaped subsurface CO_2 plumes were predicted (Supplement 1b and c), with CO_2 spreading along the top of the water table, and maximum concentrations of >0.9 mass fraction CO_2 within the cores of the plumes. Profiles of predicted surface CO_2 flux were symmetrical around the surface well trace (Supplement 1a and b) and, if extrapolated along the length of the well, would result in constant longitudinal leakage flux. The predicted width of the subsurface CO_2 plume was greater for Release 2 than 1 (Supplement 1b and d), which resulted in a wider zone of surface leakage fluxes (i.e., spreading to ~5 m from the well trace, versus to 2.5 m) (Supplement 1a and c). Maximum surface leakage fluxes simulated for Releases 1 and 2 were ~400 and 1200 g m^{-2} d^{-1}, respectively. We emphasize that the simulations were predictive, i.e., carried out before the horizontal shallow-release experiments, with permeability calibration based on the earlier vertical well injection test.

Figure 2 shows the spatio-temporal evolution of F_{CO2} measured during the timeframes of Releases 1 and 2 and Figure 3 shows the corresponding CO_2 discharges. There was no evidence of F_{CO2} related to leakage at distances >7.5 m from the well trace. Consequently, to estimate background (soil respiration) CO_2 discharge (D_{back}) for each grid dataset, we calculated the mean F_{CO2} for distances 10-30 m from the well trace, and assuming this F_{CO2} was representative of background F_{CO2} for the entire grid area, multiplied it by 7700 m^2. The CO_2 discharge associated with leakage from along the well (D_{leak}) was then estimated as $D_{tot} - D_{back}$ (Figure 3). A decrease in background F_{CO2} was observed over the two days preceding Release 1, which continued during the first day of

Release 1 when no evidence of leakage was observed at the surface (7-9 July 2007); Figures 2a-c and 3). Breakthrough of CO_2 at the surface, indicated by elevated F_{CO2}, was observed at a single point along the well trace on Day 2 of Release 1 and remained relatively stable to Day 3 (Figure 2d and e). On these days, D_{tot} remained similar to that observed on Day 1 of the release, while D_{back} decreased, and D_{leak} increased (Figure 3). Then, elevated F_{CO2} was measured at six point sources aligned along the well trace on Day 4 of the release (Figure 2f). The position of these leaks remained stable over the next six days, while the magnitude of F_{CO2} increased from Day 4 to 6, to remain relatively constant until Day 10 (Figures 2g-j and 1b). Maximum F_{CO2} was ~1600 g $m^{-2}d^{-1}$. From Day 4 to 8, D_{tot} was highly variable and did not exceed values measured prior to Release 1. Changes in D_{tot} over this time period generally followed changes in D_{back}, while D_{leak} increased to remain relatively stable at ~0.1 t d^{-1} from day 6 to 8 (Figure 3). Figure 1a and b illustrate the spatial relationship of the F_{CO2} leakage anomalies to well design. Five of the six F_{CO2} peaks measured along the well trace were located above the well packers (packers 6, 4, 3, 2, and 0) and tended to be located above the higher elevation end of the slotted well sections. An exception to this pattern is the F_{CO2} peak measured above the unslotted section on the far NE end of the well.

F_{CO2} measurements began on Day 5 of Release 2 and showed similar surface leakage patterns as those observed during Release 1 (Figures 1c and 2k and l). However, the magnitude of F_{CO2} measured along the well trace was higher (maximum = 6000 g m^{-2} d^{-1}) and a greater degree of spreading of leaking CO_2 was observed both along and away from the well trace relative to Release 1. D_{tot} and D_{leak} were ~0.45 and 0.33 t d^{-1}, respectively,

on Days 7 and 8 of Release 2, while D_{back} remained relatively low. F_{CO2}, D_{tot}, and D_{leak} showed large declines on Day 1 following the end of Release 2 and dropped to near-background values on the second day after the release (Figures 2m and n and 3).

4. Discussion and Conclusions

We present F_{CO2} measurements and numerical simulations associated with the first-ever CO_2 release experiments from a subsurface line source. Model predictions of the evolution of the surface flux leakage signals were closely matched by field measurements of F_{CO2}. For example, surface breakthrough of CO_2 was predicted to occur 1.5 days after the start of Release 1, and was observed on Day 2 (precise breakthrough time was not recorded by daily grid measurements). A rapid drop of the surface leakage signal was both predicted and observed following the end of Release 2 (Figures 2d, m, n and 3). Also, assuming that the temporal evolution of leakage CO_2 flux over the well and D_{leak} should be similar, both predicted and observed leakage signals reached near-steady state on Day 6 of Release 1 (Figure 3). Finally, the observed extent of CO_2 spreading away from the well (i.e., a maximum of 2.5 to 5 m for Release 1 and 5 to 7.5 m for Release 2) at near-steady state conditions was close to that predicted by models (Figures 2j and l and 4a and c).

As suggested by numerical models, while some CO_2 spreading likely occurred on top of the water table, little CO_2 was lost to (dissolved in) the groundwater system during the releases (Figures 4b and d). As a result, the groundwater system minimally attenuated

CO_2 flow to the surface, D_{leak} values on Days 6-8 of Release 1 and Days 7-8 of Release 2 were close to CO_2 release rates (Figure 3), and CO_2 spreading away from the well was limited. Also, the relatively fast predicted and observed breakthrough time of CO_2 to the surface during Release 1 and decline of F_{CO2} to near-background values following the end of Release 2 were likely due in part to high soil permeability caused by macropores allowing for rapid exchange of soil and atmospheric gases.

There were key differences between predicted and observed leakage flux signals. First, numerical simulations were oriented transverse to the well and therefore did not model the observed multiple point-source leakage signals aligned along the well trace, which showed some connection to one another on Days 7 and 8 of Release 2 (Figures 1 and 2). Second, the maximum predicted leakage fluxes above the well were lower than those measured during Releases 1 and 2 due to the longitudinal averaging implicit in the 2D transverse model. The spatial distribution of observed leakage fluxes was strongly correlated with the well design (Figure 1). CO_2 likely flowed from relatively low to high elevation within the well injection zones until it encountered the barriers of packers 6, 4, 3, 2, and 0. It probably then flowed upward to the surface, leading to concentrated areas of relatively high-magnitude surface leakage. Unmapped zones of high soil permeability may have further focused CO_2 flow. The far NE F_{CO2} peak measured above the unslotted well section was likely due to CO_2 flow to the surface along the outside of the well bore, an unexpected process not included in the numerical model. Higher vertical pressure gradients were probably established by the higher CO_2 release rate of Release 2, leading to more direct flow of CO_2 from its release points to the surface and a more

longitudinally continuous surface leakage signal, relative to Release 1. While the intent of the release experiments was to create a longitudinally uniform leakage pattern, the effects of well design and soil physical properties likely created signals more realistic of leakage along partially-sealed faults or fractures, where fluids migrate through discrete pathways to the surface. Leakage along such features may actually be more likely at sites selected for CO_2 storage, where, if present, faults will probably be inactive and largely sealed.

The grid used for chamber measurements included measurement points close to and away from the horizontal well, allowing us to quantify CO_2 emissions from background soil respiration processes separately from leakage. We observed relatively high D_{back} on 7 July 2007, followed by a decrease at about the same rate as the increase in D_{leak} (Figure 3). Consequently, D_{tot} was variable during Release 1, but did not exceed values measured prior to the release. A rainstorm occurred on the evening of 6 July 2007, during otherwise dry and hot (average daytime temperature = 22^{o}C) weather conditions. The decrease in D_{back} following the rainstorm was likely due to a decline in soil moisture content and associated plant and microbial activity. A primary challenge of near-surface detection of potential CO_2 leakage from geologic storage sites is to discern a leakage signal within background CO_2 variability. This could be difficult if the signal is of very small magnitude and/or spatial extent [e.g., *Lewicki et al.*, 2005]. Both Releases 1 and 2 resulted in high-magnitude leakage relative to background CO_2 fluxes, but the overall areas of the anomalies were small relative to the grid area. As a result, when background F_{CO2} is high (e.g., during the growing season, or after rain events during dry periods), it

can mask leakage F_{CO2}. This effect was clear during Release 1, when considering D_{tot}, and would be stronger if one were attempting to detect leakage signals within a larger, reservoir-scale area. Since background F_{CO2} was relatively low during Release 2, D_{tot} was clearly discernable from D_{back} measured prior to Release 1. Because the point-measurement nature of the chamber method allows mapping of the spatial distribution of F_{CO2} and we measured F_{CO2} on a spatial scale fine enough to capture the leakage signal, leakage was visible in F_{CO2} maps during both Releases 1 and 2 (Figure 2). Use of a CO_2 measurement technique, however, that averages over a relatively large area (e.g., eddy covariance) would likely have rendered CO_2 leakage detection during Release 1 difficult. Our results emphasize the importance of (1) careful characterization of background CO_2 variability prior to CO_2 injection into the storage reservoir, (2) limitation of the total area of investigation by focus on features most susceptible to leakage (e.g., wells, faults), and (3) use of a variety of complementary CO_2 measurement techniques in a program of storage site monitoring. Overall, the new ZERT CO_2 release facility provides an excellent opportunity to study CO_2 migration processes in the near-surface environment and develop integrated field methodologies to detect and quantify potential CO_2 leakage from geologic storage sites.

Acknowledgements

We thank G.E. Hilley and M.L. Fischer for valuable input and advice. This work was funded by the Assistant Secretary for Fossil Energy, Office of Sequestration, Hydrogen, and Clean Coal Fuels, NETL, of the U.S. Dept. of Energy under Contract No. DE-AC02-05CH11231.

References

Chiodini, G., G.R. Cioni, M. Guidi, B. Raco, and L. Marini (1998), Soil CO_2 flux measurements in volcanic and geothermal areas, *Appl. Geochem., 13*, 543–552.

Deutsch, C.V. and A.G. Journel (1998), GSLIB, geostatistical software library and users guide, Oxford Univ Press, New York.

Evans, W.C., M.L. Sorey, B.M. Kennedy, D.A. Stonestrom, J.D. Rogie, and D.L. Shuster (2001), High CO_2 emissions through porous media: transport mechanisms and implications for flux measurement and fractionation, *Chem. Geol., 177*, 15-29.

International Energy Agency (1997), Carbon Dioxide Utilization, IEA Greenhouse Gas R and D Programme, Paris.

International Energy Agency (2004), Prospects for CO_2 Capture and Storage, IEA Publications, Paris.

IPCC (2005), IPCC Special Report on Carbon Dioxide Capture and Storage, Cambridge University Press, Cambridge.

Lewicki, J.L., G.E. Hilley, and C.M. Oldenburg (2005), An improved strategy to detect CO_2 leakage for verification of geologic carbon sequestration, *Geophys. Res. Lett., 32,* L19403, doi:10.1029/2005GL024281.

Lewicki, J.L., D. Bergfeld, C. Cardellini, G. Chiodini, D. Granieri, N. Varley, and C. Werner (2005), Comparative soil CO_2 flux measurements and geostatistical estimation methods on Masaya volcano, Nicaragua, *Bull. Volcanol., 68,* 76-90.

Oldenburg, C.M. and A.J.A. Unger (2003), On leakage and seepage from geologic carbon sequestration sites: unsaturated zone attenuation, *Vadose Zone J.*, *2*, 287-296.

Oldenburg, C.M. and A.J.A. Unger (2004), Coupled vadose zone and atmospheric surface-layer transport of CO_2 from geologic carbon sequestration sites, *Vadose Zone J.*, *3*, 848–857.

Pruess, K., C. Oldenburg, and G. Moridis (1999), TOUGH2 User's Guide, Version 2.0, *Lawrence Berkeley National Laboratory Report LBNL-43134*.

Table 1. Properties of two-dimensional transverse model of shallow release.

	Soil	Cobble
Porosity	0.35	0.35
Permeability	5×10^{-11} m^2	3.2×10^{-12} m^2
Capillary Pressure	van Genuchten[1] $\lambda = 0.291$, $S_{lr} = 0.15$, $\alpha = 2.04 \times 10^{-4}$ Pa^{-1}, $P_{max} = 5 \times 10^5$ Pa, $S_{ls} = 1$.	van Genuchten[1] $\lambda = 0.627$, $S_{lr} = 0.10$, $\alpha = 1.48 \times 10^{-3}$ Pa^{-1}, $P_{max} = 5 \times 10^5$ Pa, $S_{ls} = 1$.
Relative permeability	van Genuchten[1] $S_{lr} = 0.17$, $S_{gr} = 0.05$	van Genuchten[1] $S_{lr} = 0.12$, $S_{gr} = 0.05$
Molec. diffusivity	Liquid: 10^{-10} m^2 s^{-1} Gas: 10^{-5} m^2 s^{-1}	Liquid: 10^{-10} m^2 s^{-1} Gas: 10^{-5} m^2 s^{-1}

[1]*Pruess et al.,* 1999.

Figure Captions

Figure 1. (a) Surface and horizontal well elevation. Black squares are packers numbered 0-6. Plots of F_{CO2} measured along the surface well trace on (b) 17-18 July 2007 and (c) 7-8 August 2007. Distance = 0 m corresponds to grid origin shown in Figure 2.

Figure 2. Log F_{CO2} maps for measurements made on (a-j) 7-16 July 2007 and (k-n) 9-12 August 2007. Black dots show measurement locations. White circles show grid origin. White line in (a) shows approximate surface well trace.

Figure 3. Plot of CO_2 discharge versus time for Releases 1 and 2. D_{tot} (black dots), D_{back} (open circles), and D_{leak} (black squares) are total, background (soil respiration), and leakage discharges, respectively. Black line shows simulated time evolution of leakage CO_2 flux directly over well.

Supplement 1. (a) Surface profile of simulated leakage CO_2 flux across well and (b) corresponding cross-section of simulated subsurface CO_2 concentrations (mass fraction in the gas phase) for Release 1, Day 8. Black circle is cross section of horizontal well and white lines are contours of liquid saturation (contour interval = 0.2). (c) Surface profile of simulated leakage CO_2 flux across well and (d) corresponding cross-section of subsurface CO_2 concentrations for Release 2, Day 8.

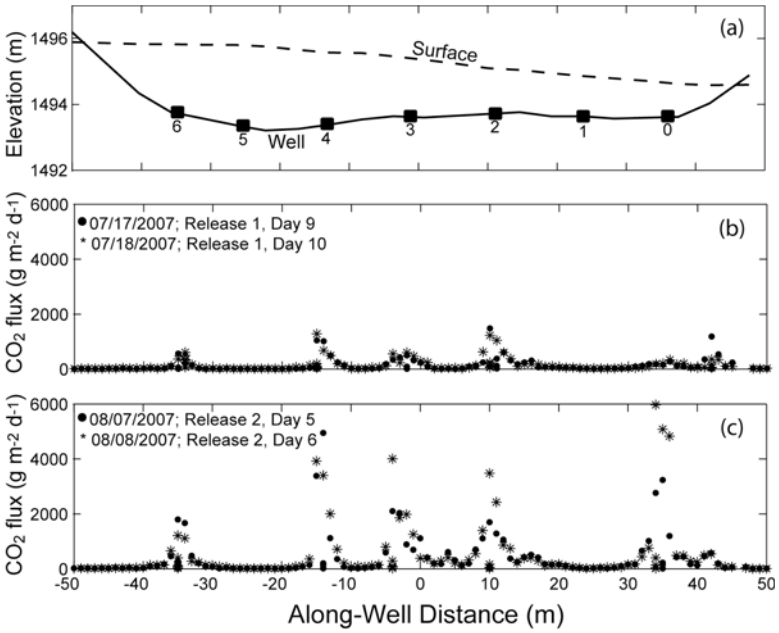

Figure 1. (a) Surface and horizontal well elevation. Black squares are packers numbered 0-6. Plots of F_{CO2} measured along the surface well trace on (b) 17-18 July 2007 and (c) 7-8 August 2007. Distance = 0 m corresponds to grid origin shown in Figure 2.

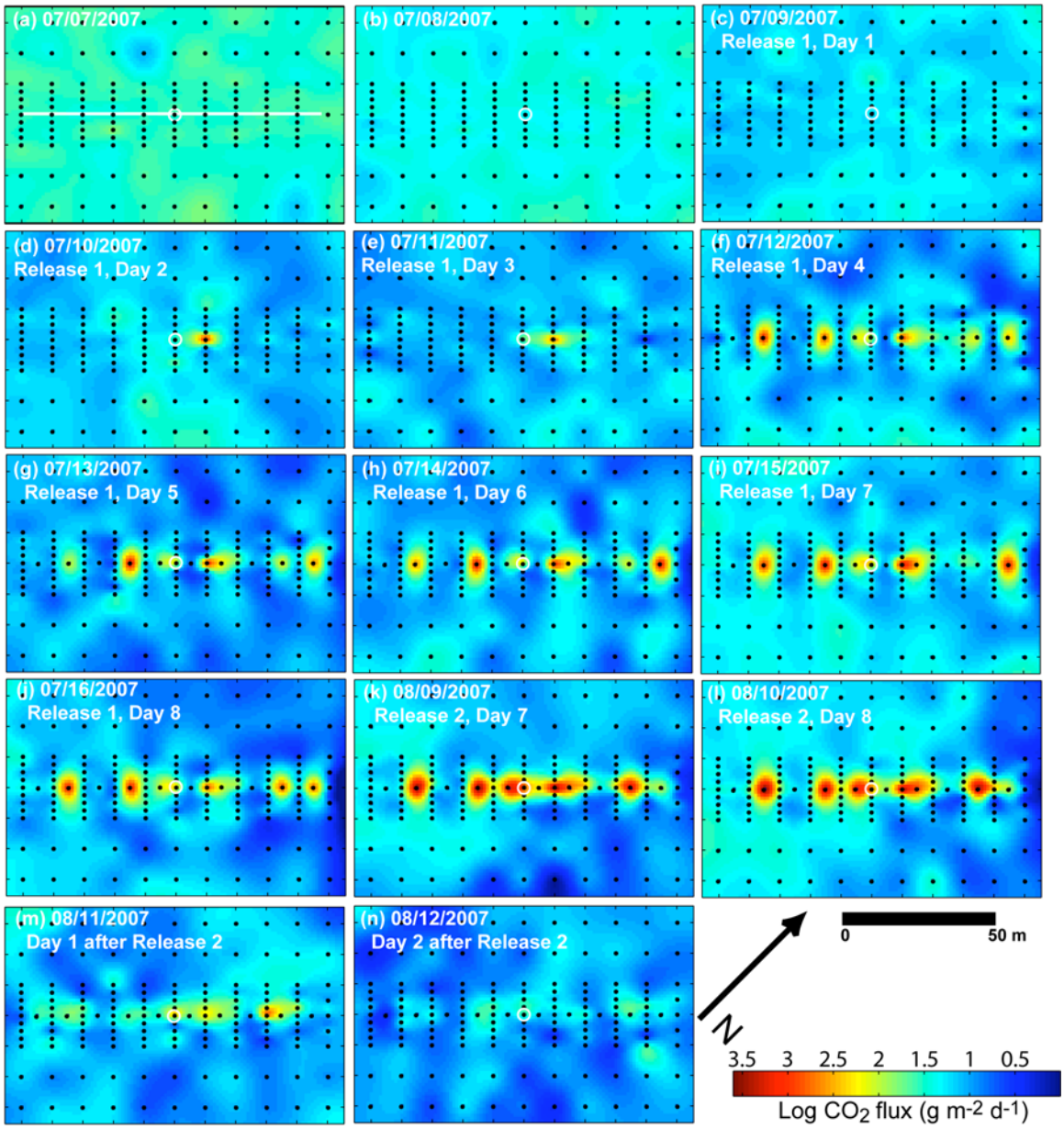

Figure 2. Log F_{CO2} maps for measurements made on (a-j) 7-16 July 2007 and (k-n) 9-12 August 2007. Black dots show measurement locations. White circles show grid origin. White line in (a) shows approximate surface well trace.

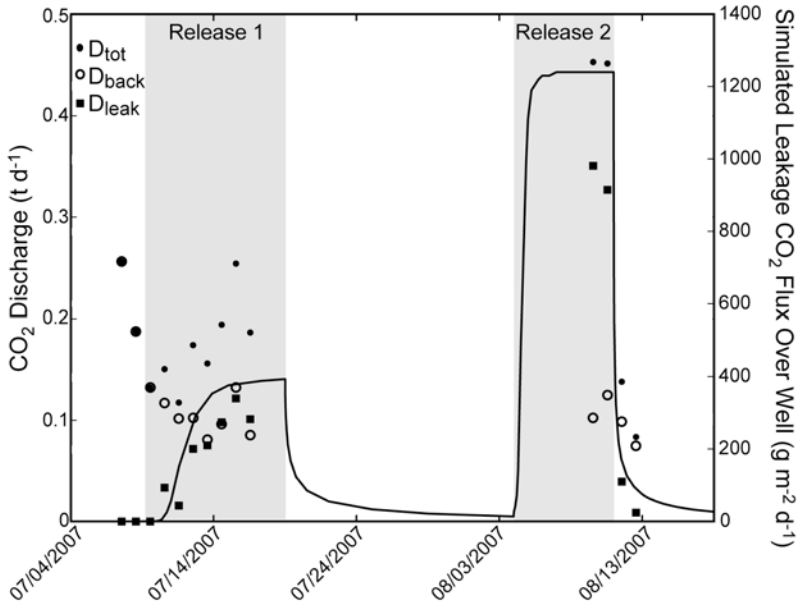

Figure 3. Plot of CO_2 discharge versus time for Releases 1 and 2. D_{tot} (black dots), D_{back} (open circles), and D_{leak} (black squares) are total, background (soil respiration), and leakage discharges, respectively. Black line shows simulated time evolution of leakage CO_2 flux directly over well.

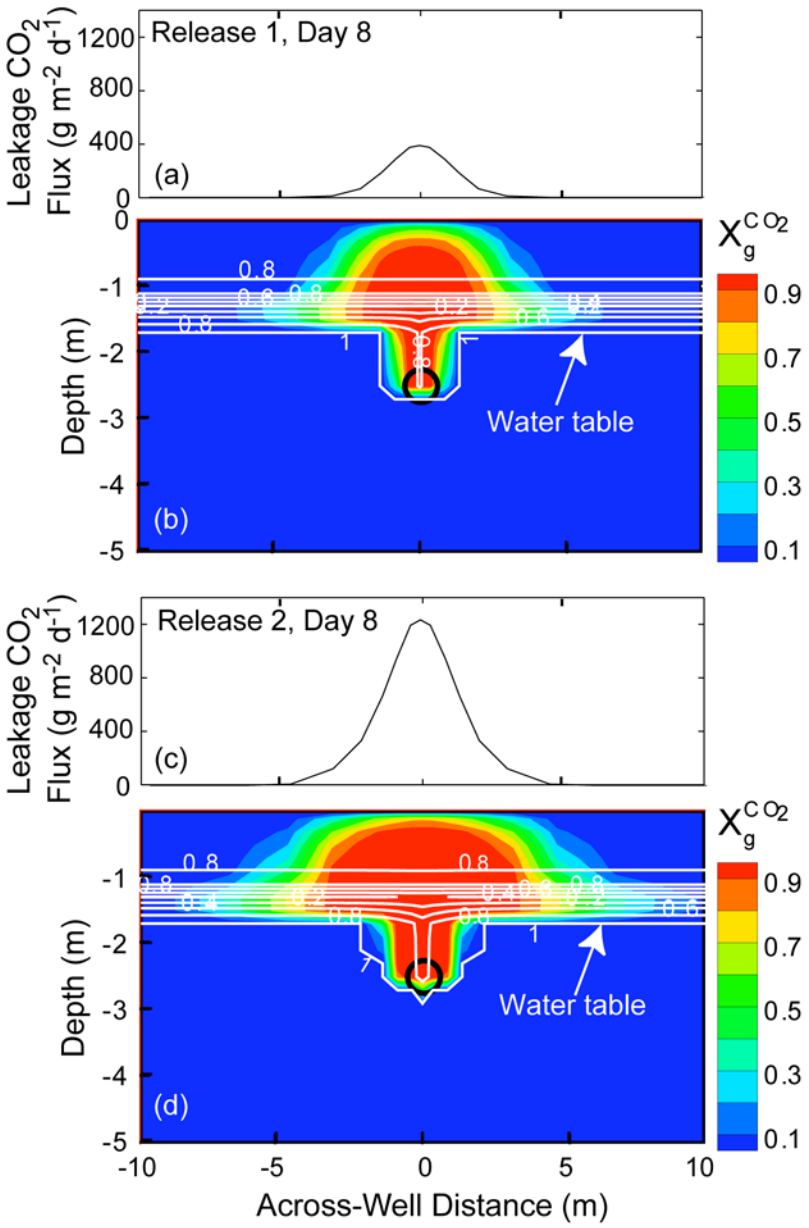

Supplement 1. (a) Surface profile of simulated leakage CO_2 flux across well and (b) corresponding cross-section of simulated subsurface CO_2 concentrations (mass fraction in the gas phase) for Release 1, Day 8. Black circle is cross section of horizontal well and white lines are contours of liquid saturation (contour interval = 0.2). (c) Surface profile of simulated leakage CO_2 flux across well and (d) corresponding cross-section of subsurface CO_2 concentrations for Release 2, Day 8.